Superhydrophobic Sand：A Hope for Desert Water Storage and Transportation Project

Liwei Chen[a], Yifan Si[a], Zhiguang Guo[ab]*, and Weimin Liu[b]

[a] Hubei Collaborative Innovation Centre for Advanced Organic Chemical Materials and Ministry of Education Key Laboratory for the Green Preparation and Application of Functional Materials, Hubei University, Wuhan 430062, People's Republic of China.

[b] State Key Laboratory of Solid Lubrication, Lanzhou Institute of Chemical Physics, Chinese Academy of Sciences, Lanzhou 730000, People's Republic of China

*Corresponding author: zguo@licp.cas.cn (Z. G. G.)

Supporting Figures

1. Materials preparation

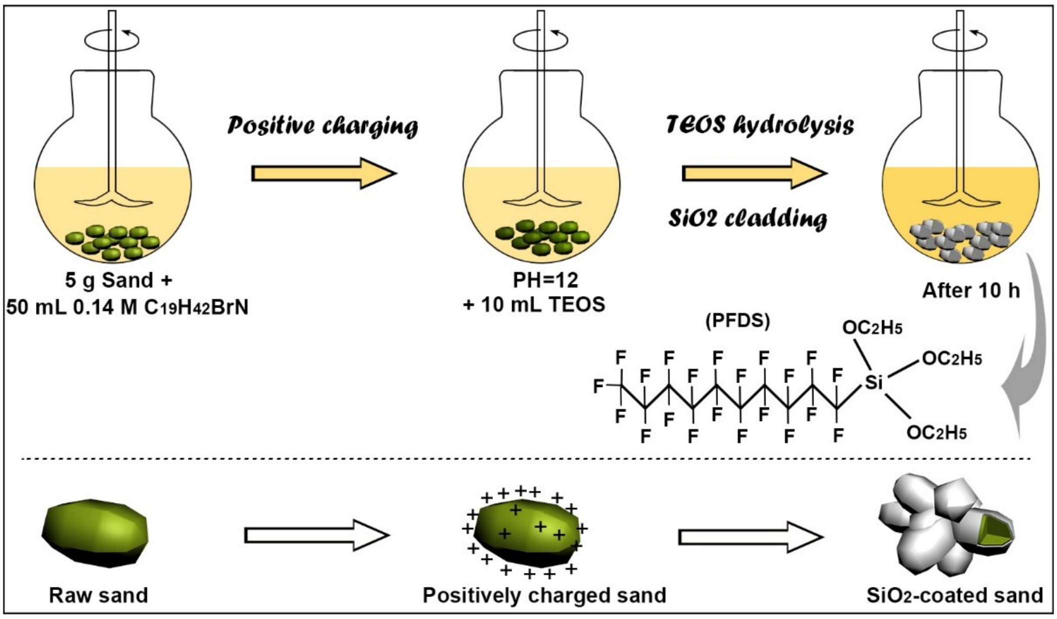

Supplementary Fig. S1. Schematic illustrating the preparation process of SiO_2-coated superhydrophobic sand (sand@SiO_2), including the positive charging treatment of sand, hydrolysis of tetraethoxysilane (TEOS) in alkaline environment, SiO_2 cladding on sand surfaces, and final modification with 1H, 1H, 2H, 2H-Perfluorodecyltriethoxysilane (PFDS). To successfully coat SiO_2 on sand surface, the raw sand is pre-treated with cetyltrimethylammonium bromide (CTAB) for positive charging.

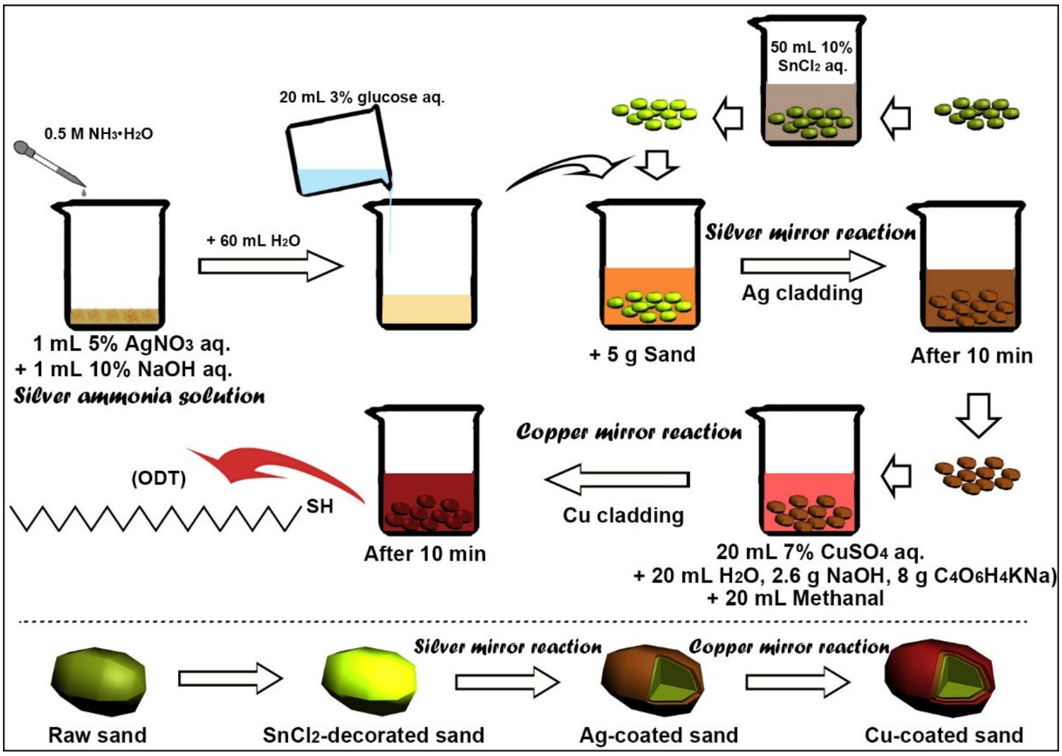

Supplementary Fig. S2. Schematic illustrating the preparation process of Ag and Cu-coated superhydrophobic sand (sand@Ag and sand@Ag@Cu), including the decoration of $SnCl_2$, silver mirror reaction for Ag cladding on sand surface, copper mirror reaction for Cu cladding on sand surface, and final modification with n-octadecanethiol (ODT). In order to successfully cladding the sand with metal Ag, the raw sand is pre-treated with stannous chloride ($SnCl_2$) for catalytic action.

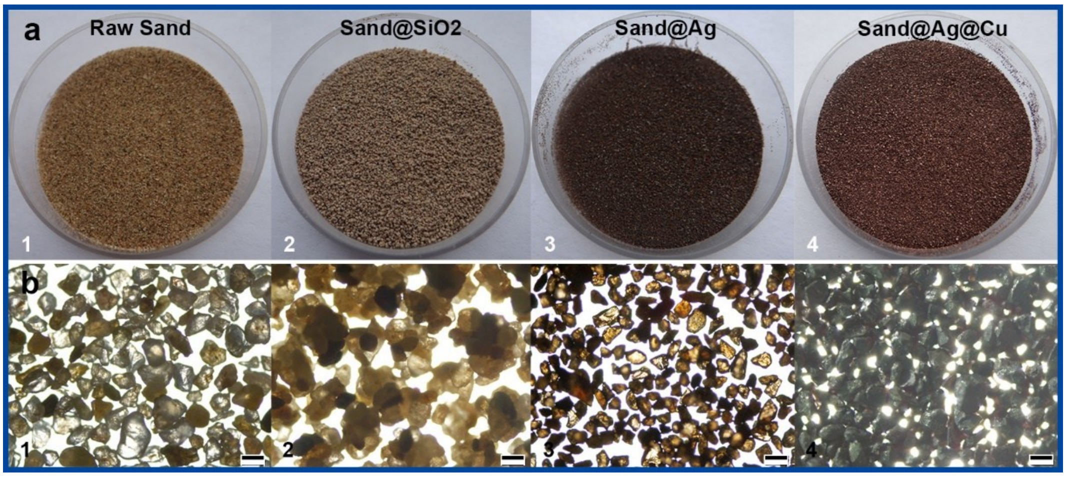

Supplementary Fig. S3. a) Optical photographs of (a$_{-1}$) raw sand and prepared (a$_{-2}$) sand@SiO_2, (a$_{-3}$) sand@Ag and (a$_{-4}$) sand@Ag@Cu particles; b) Optical microscope images of (b$_{-1}$) raw sand and prepared (b$_{-2}$) sand@SiO_2, (b$_{-3}$) sand@Ag and (b$_{-4}$) sand@Ag@Cu particles. The scale bar is 200 μm.

2. Energy dispersive X-ray spectroscopy (EDXS) results

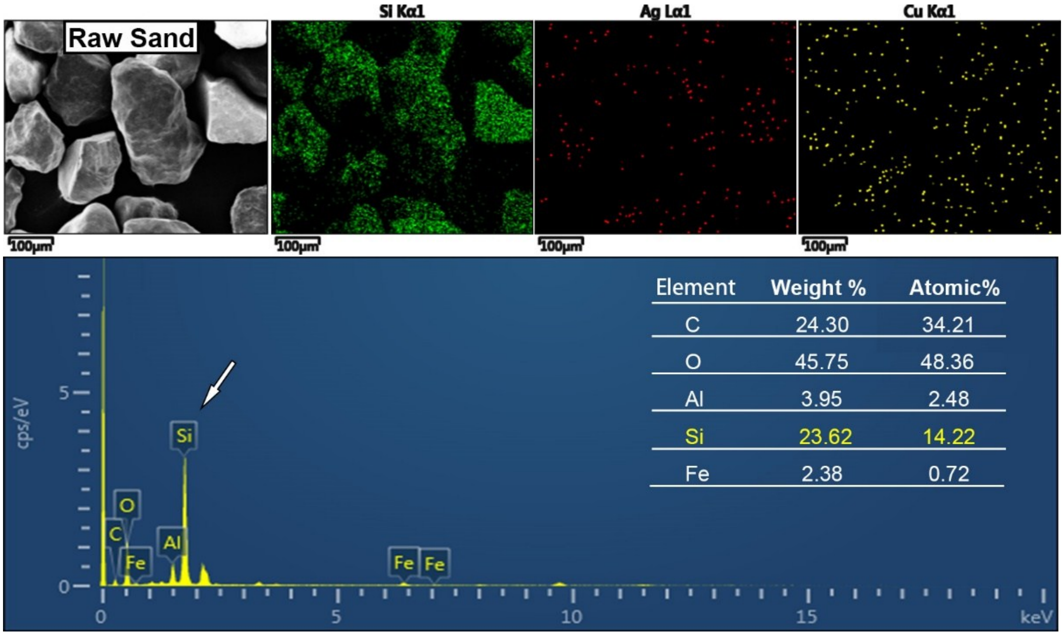

Element	Weight %	Atomic%
C	24.30	34.21
O	45.75	48.36
Al	3.95	2.48
Si	23.62	14.22
Fe	2.38	0.72

Supplementary Fig. S4. EDXS results of the raw sand particles.

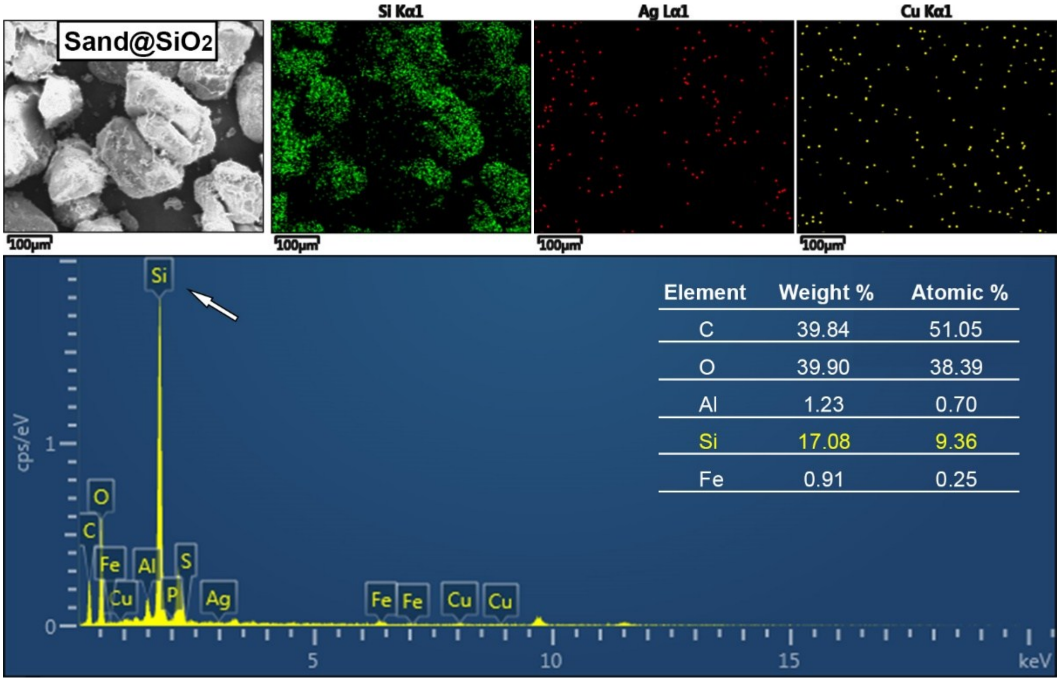

Element	Weight %	Atomic %
C	39.84	51.05
O	39.90	38.39
Al	1.23	0.70
Si	17.08	9.36
Fe	0.91	0.25

Supplementary Fig. S5. EDXS results of the sand@SiO_2 particles.

From the Fig. S4–7, one can see the element content and distribution of Si, Ag and Cu. First, the main component of raw sand is silicate, and several metal elements (*e.g.*, Al, Fe) are also contained in sand, as shown in Fig. S4. After cladding a SiO_2 outlayer (sand@SiO_2), the element distributions have little changes, but the absorption peak of Si becomes more evident (Fig. S5).

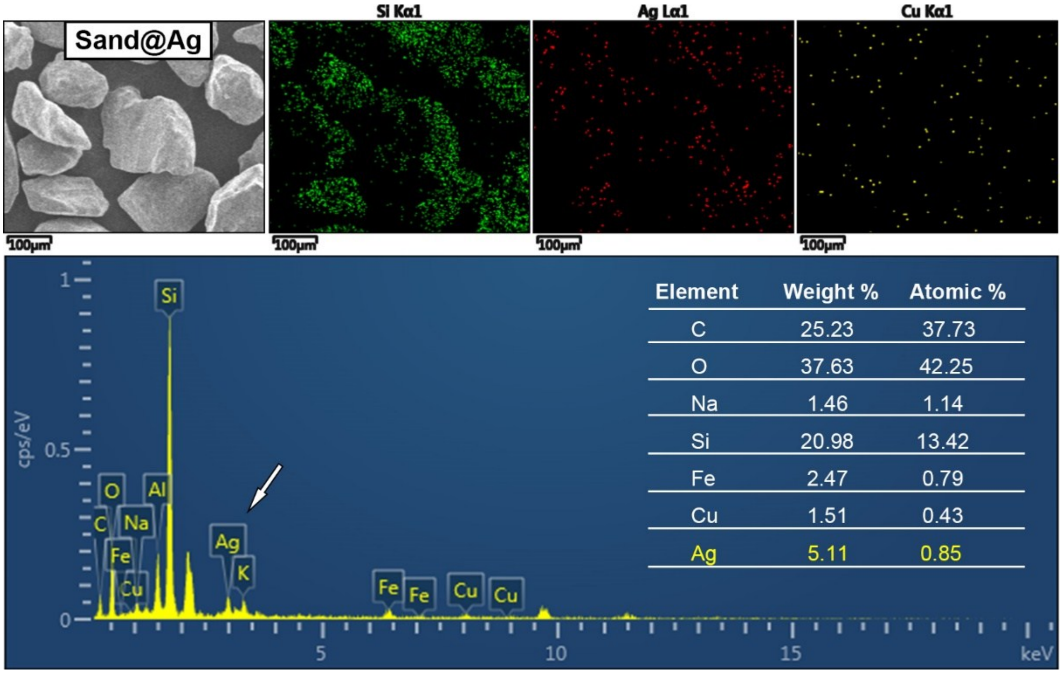

Element	Weight %	Atomic %
C	25.23	37.73
O	37.63	42.25
Na	1.46	1.14
Si	20.98	13.42
Fe	2.47	0.79
Cu	1.51	0.43
Ag	5.11	0.85

Supplementary Fig. S6. EDXS results of the sand@Ag particles.

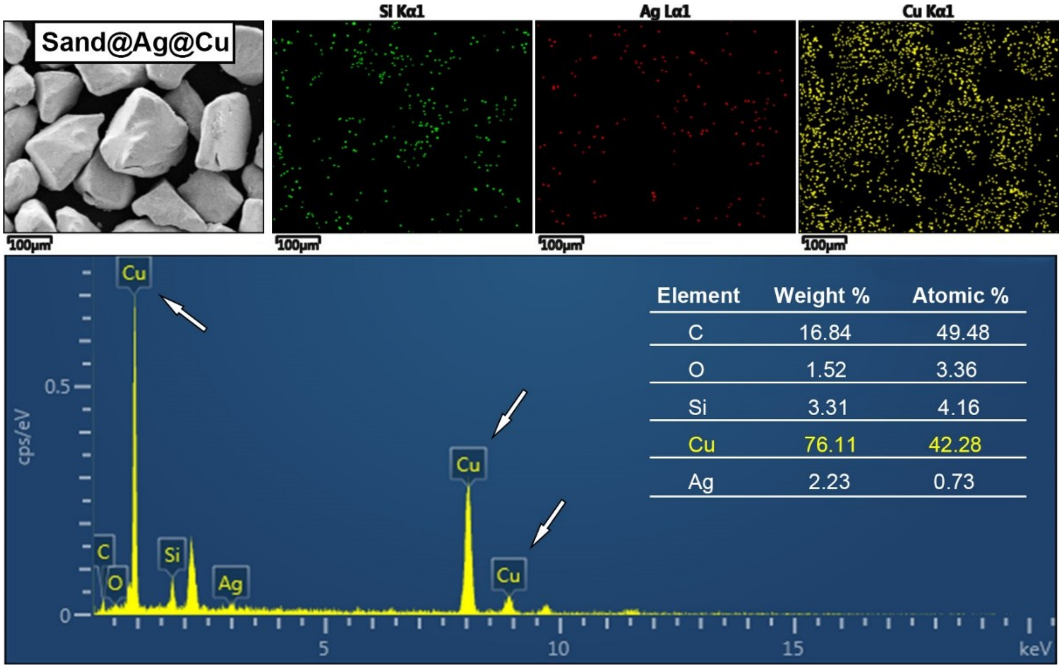

Element	Weight %	Atomic %
C	16.84	49.48
O	1.52	3.36
Si	3.31	4.16
Cu	76.11	42.28
Ag	2.23	0.73

Supplementary Fig. S7. EDXS results of the sand@Ag@Cu particles.

When cladding an Ag outlayer (sand@Ag), the most obvious changes are that the content of Ag is higher and the distribution of Ag is more obvious (Fig. S6). Next, we go a step further, cladding a Cu outlayer on sand@Ag (sand@Ag@Cu). The result clearly shows that the content and distribution of Cu significantly increase (Fig. S7). The EDXS results are consistent with our experimental expectations, implying the successful coating of Si, Ag and Cu on sand.

3. Fourier transformer infrared spectra (FTIR) results

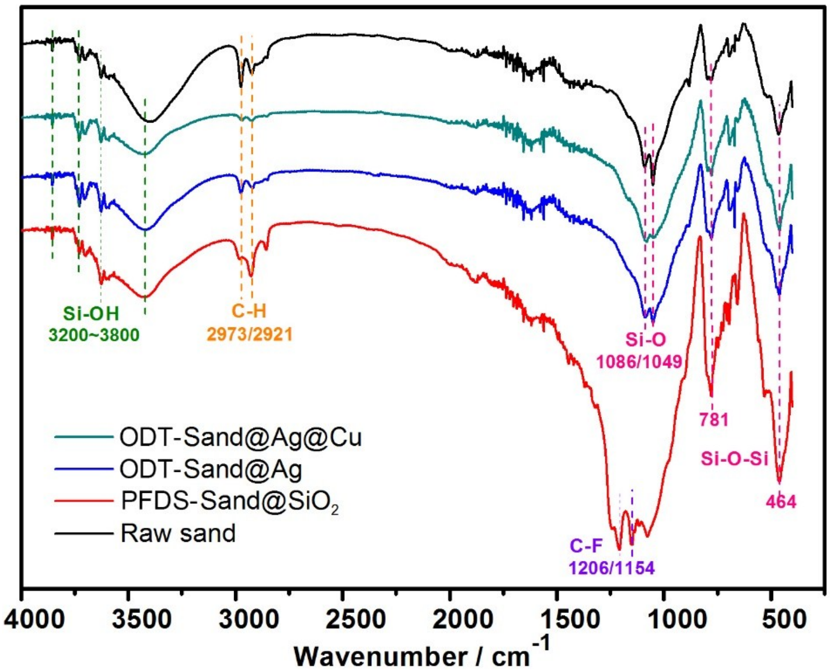

Supplementary Fig. S8. Infrared absorption spectra of the raw sand, the sand@SiO$_2$ modified with PFDS, the sand@Ag and sand@Ag@Cu modified with ODT.

The bands at 3200–3800 cm^{-1} are assigned to Si–OH groups. The absorption peaks at 2973 and 2921 cm^{-1} are attributed to the stretching vibration of C–H in CH$_3$ and CH$_2$ groups. The absorption peaks at 1086 and 1049 cm^{-1} are attributed to the Si–O group, and the bands below 1000 cm^{-1} are attributed to the vibrations of Si–O–Si bonds. Especially, it is obvious that the sand@SiO$_2$ is coated with PFDS because of the absorption peaks of C–F groups appearing at 1206 and 1154 cm^{-1}.

4. Wetting properties

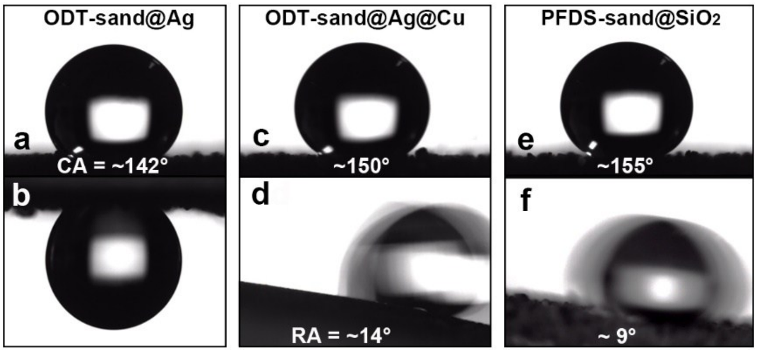

Supplementary Fig. S9. Water contact angle (CA) and rolling angle (RA) of prepared (a, b) ODT-sand@Ag, (c, d) ODT-sand@Ag@Cu, and (e, f) PFDS-sand@SiO_2 particle surfaces. The volume of water droplet is ~8 μL.

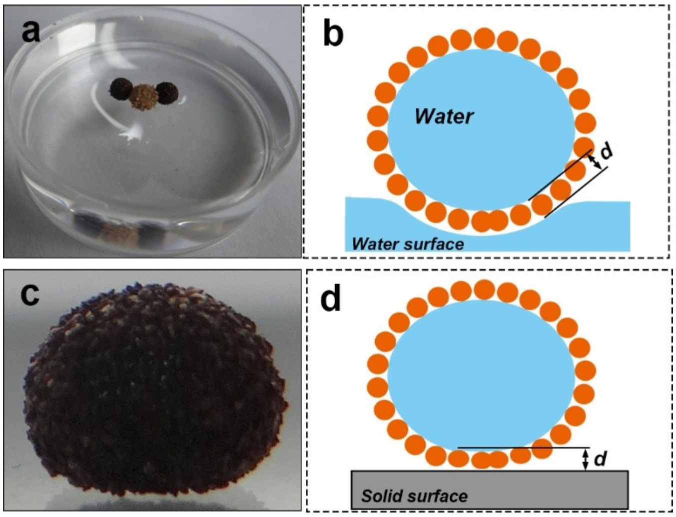

Supplementary Fig. S10. a) Photograph and b) schematic of liquid marbles floating on water surface; c) Photograph and d) schematic of liquid marbles placed on glass substrate. The liquid marbles formed by 8 μL water droplet and superhydrophobic sand. Compared with other superhydrophobic nanoparticles, the micron-scaled superhydrophobic sand can form stable liquid marbles that can stay on either water surface or sold surface without rupture.

5. Water-absorbing capacity of the raw sand

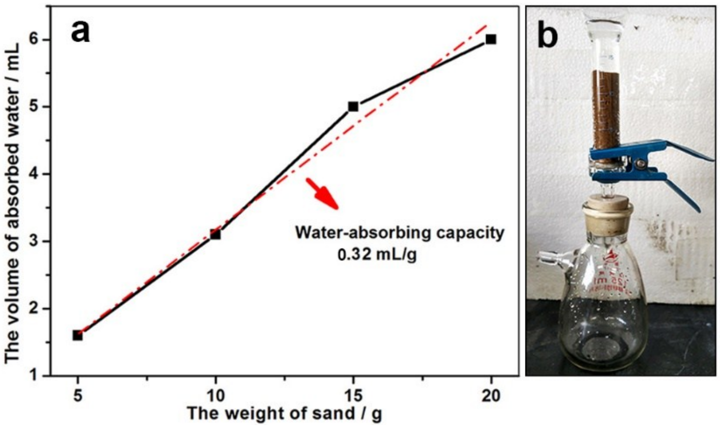

Supplementary Fig. S11. a) Water-absorbing capacity of the raw sand with increasing weight of sand, resulting in a water-absorbing capacity of ~0.32 mL/g. b) The water-absorbing test apparatus.

6. Thermal stability analysis

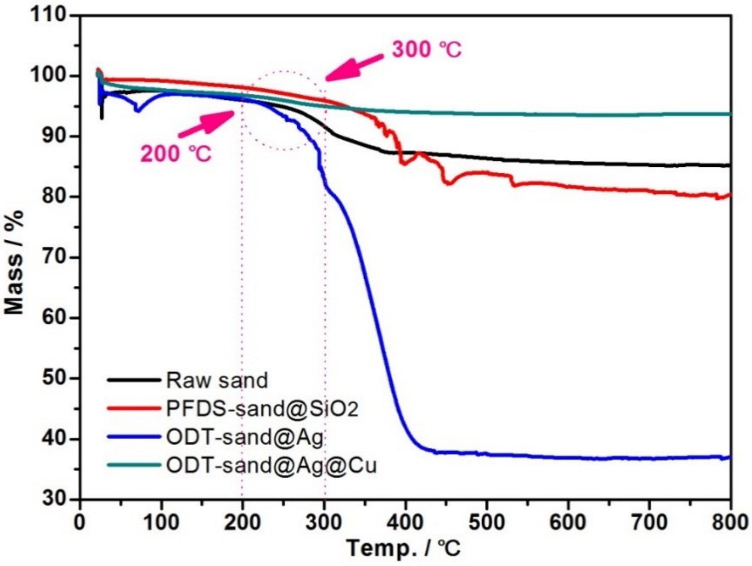

Supplementary Fig. S12. Thermogravimetric analysis (TGA) results of raw sand, PFDS-sand@SiO_2, ODT-sand@Ag and ODT-sand@Ag@Cu particles using a dynamic heating rate of 10 °C min^{-1} under the atmosphere of nitrogen. The results show that the minimum thermal decomposition temperature is at 200~300 °C and imply that these particles are usable below 200 °C.

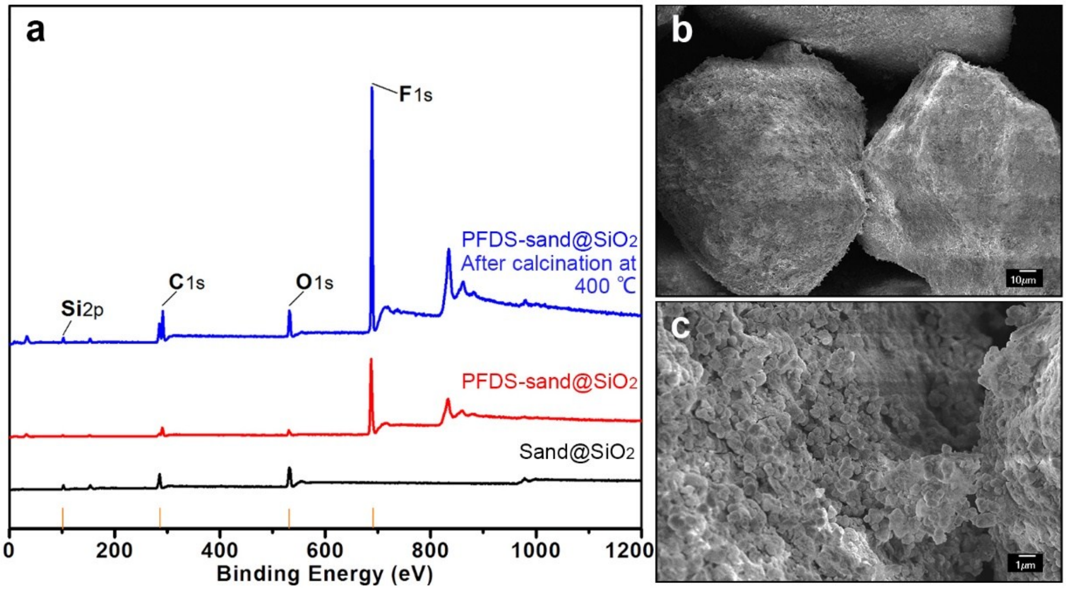

Supplementary Fig. S13. a) XPS results comparison of calcined PFDS-sand@SiO_2 particles with sand@SiO_2 and PFDS-sand@SiO_2 particles; b and c) SEM images of PFDS-sand@SiO_2 particles after calcination at 400 °C. From the results, one can see that the surface components and micro/nanostructures are well reversed after calcination.

Supporting Movies

Supplementary Movie S1. Stimulated water transportation on the sand channels made of unfixed raw sand and superhydrophobic PFDS-sand@TiO_2 particles. The movie is played at 1x speed.

Supplementary Movie S2. Stimulated water transportation on the channel adhered with raw sand particles. The movie is played at 1x speed.

Supplementary Movie S3. Stimulated water transportation on the channel adhered with hydrophobic ODT-sand@Ag particles. The movie is played at 1x speed.

Supplementary Movie S4. Anti-flow-dragging test on the inclined channel adhered with superhydrophobic ODT-sand@Ag@Cu particles at different inclined angles. The movie is played at 1x speed.

Supplementary Movie S5. Anti-flow-dragging test on the inclined channel adhered with superhydrophobic PFDS-sand@SiO_2 particles at different inclined angles. The movie is played at 1x speed.